iScience, Volume *26*

Supplemental information

Hydrochlorothiazide-induced glucose metabolism disorder is mediated by the gut microbiota via LPS-TLR4-related macrophage polarization

Jian-Quan Luo, Huan Ren, Man-Yun Chen, Qing Zhao, Nian Yang, Qian Liu, Yong-Chao Gao, Hong-Hao Zhou, Wei-Hua Huang, and Wei Zhang

Supplementary Figures

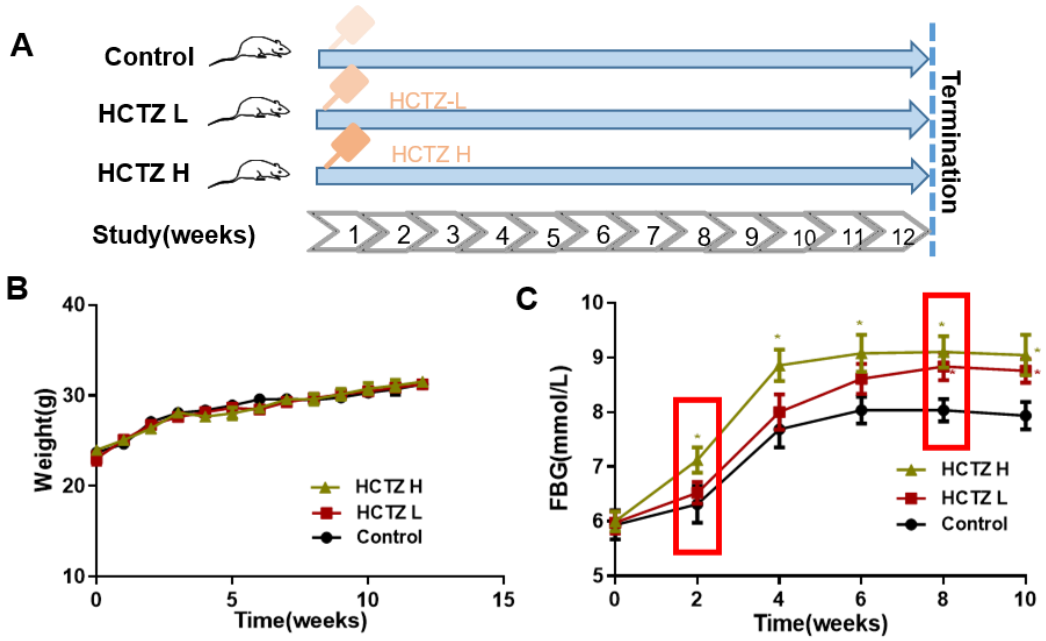

Figure S1. The adequate dosage screening of HCTZ, related to Figure 1.

(A) Schematic of HCTZ treatment of mice (n = 5-8 per group).

(B) Weight and (C) FBG in mice treated with different dosage of HCTZ (n = 5-8 per group).

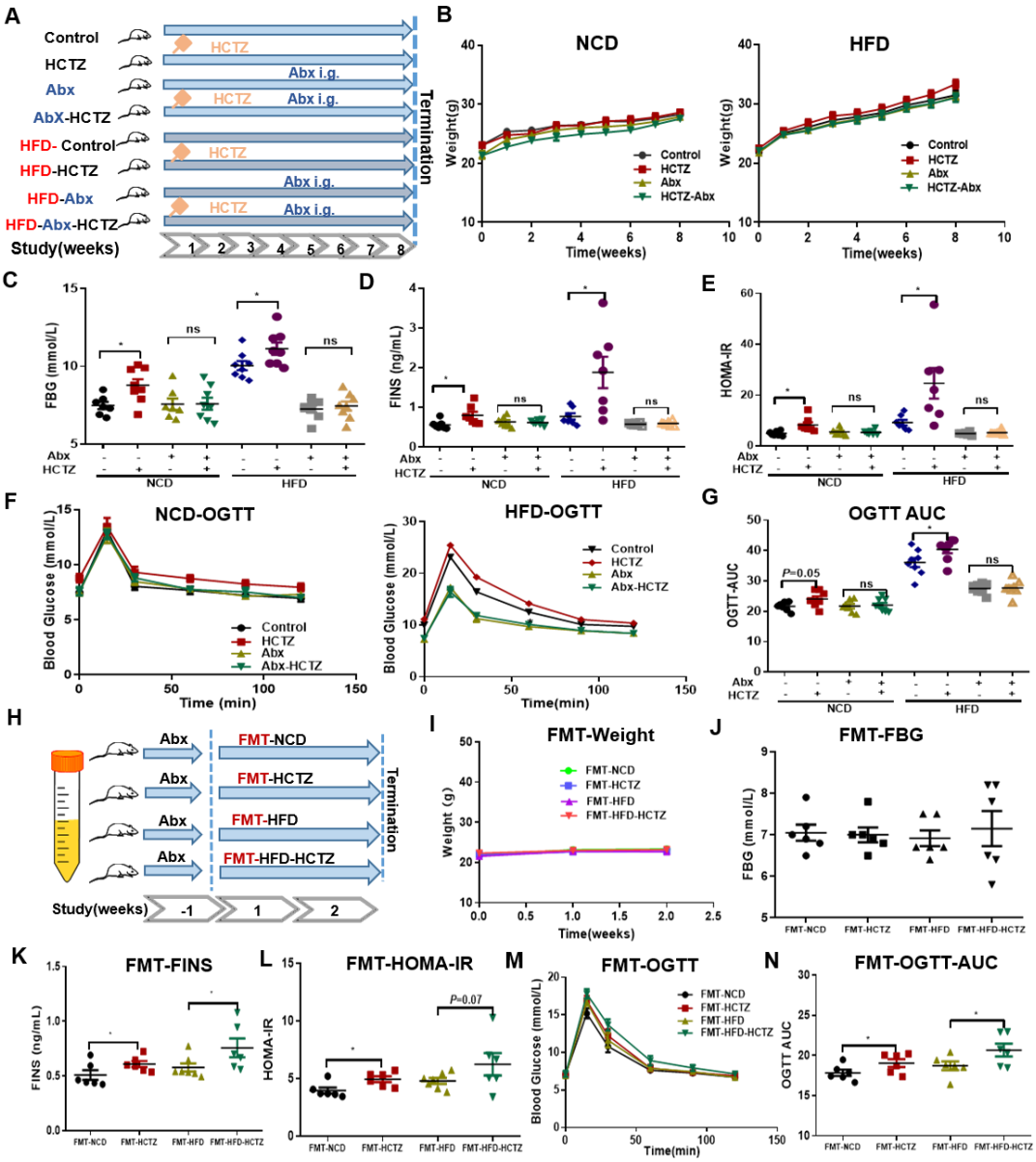

Figure S2. HCTZ -induced glucose intolerance was mediated by gut microbiota, related to Figure 1.

(A) Schematic of Abx-treated mice.

(B)-(G) Weight (B), FBG(C), FINS(D), HOMA-IR(E) and OGTT (F) and OGTT-AUC(G) of Abx-treated mice (n = 5-8 per group).

(H) Schematic of FMT experiment (n = 6-8 per group).

(I)-(N) Weight (I), FBG(J), FINS(K), HOMA-IR(L) and OGTT(M) and OGTT-AUC(N) of recipient mice in FMT experiment (n = 6-8 per group). *P<0.05.

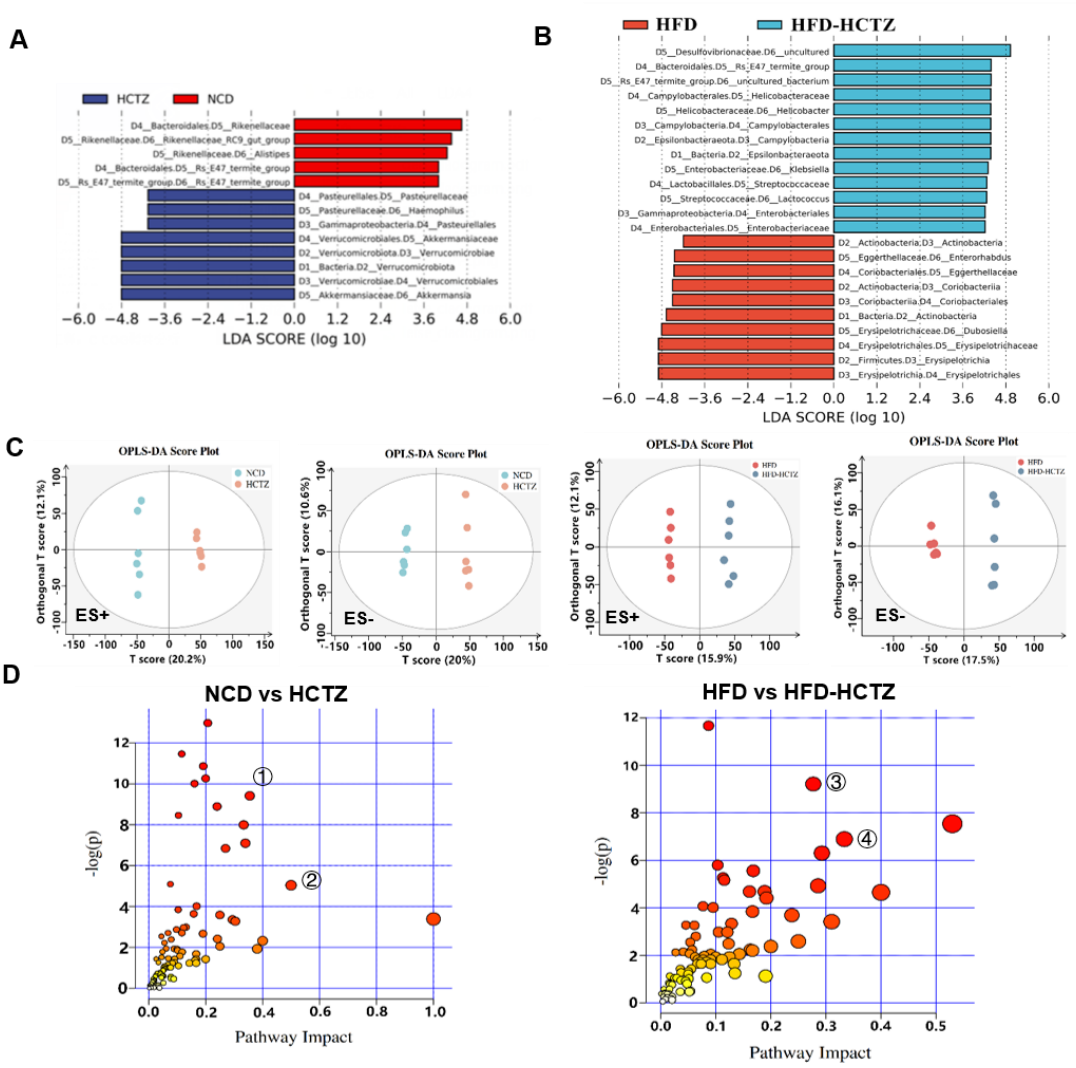

Figure S3. HCTZ consumption Changed the profiles of Gut Microbiota and plasma metabolome, related to Figure 2.

(A) Linear discriminant analysis of effect size (LEfSe) analyses HCTZ-induced clustering effect between NCD and HCTZ groups.

(B) Linear discriminant analysis of effect size (LEfSe) analyses HCTZ-induced clustering effect between HFD and HFD-HCTZ groups.

(C) Orthogonal projections to latent structures (OPLS) model exhibited a significant differentiation of plasma metabolome between HCTZ and vehicle control under normal chow diet and high-fat diet.

(D) Kyoto Encyclopedia of Genes and Genomes (KEGG) pathway enrichment analyses of the most significantly changed metabolic pathways according to untargeted metabolite profiling of plasma samples. ①Valine, leucine and isoleucine biosynthesis; ②mTOR signaling pathway; ③ Arginine and proline metabolism; ④ D-Arginine and D-ornithine metabolism.

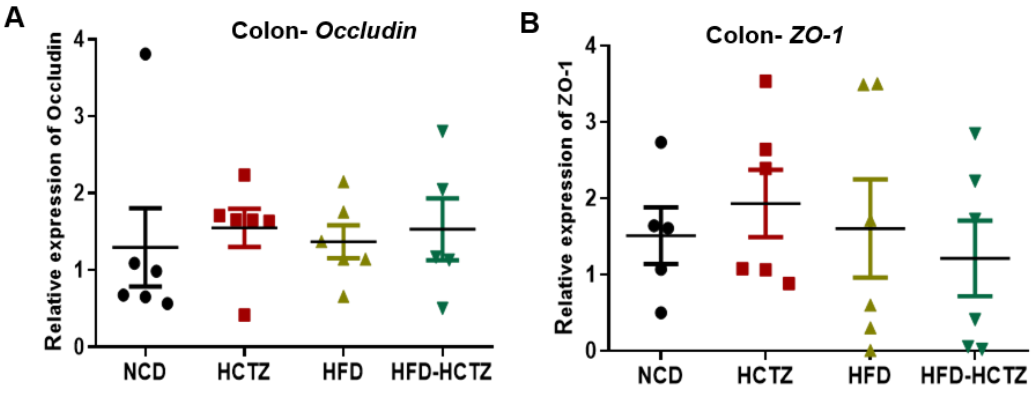

Figure S4. The effect of HCTZ on tight-junction proteins in colon. HCTZ makes no difference on ZO-1 (A) and Occludin (B) expression in colon, related to Figure 3.

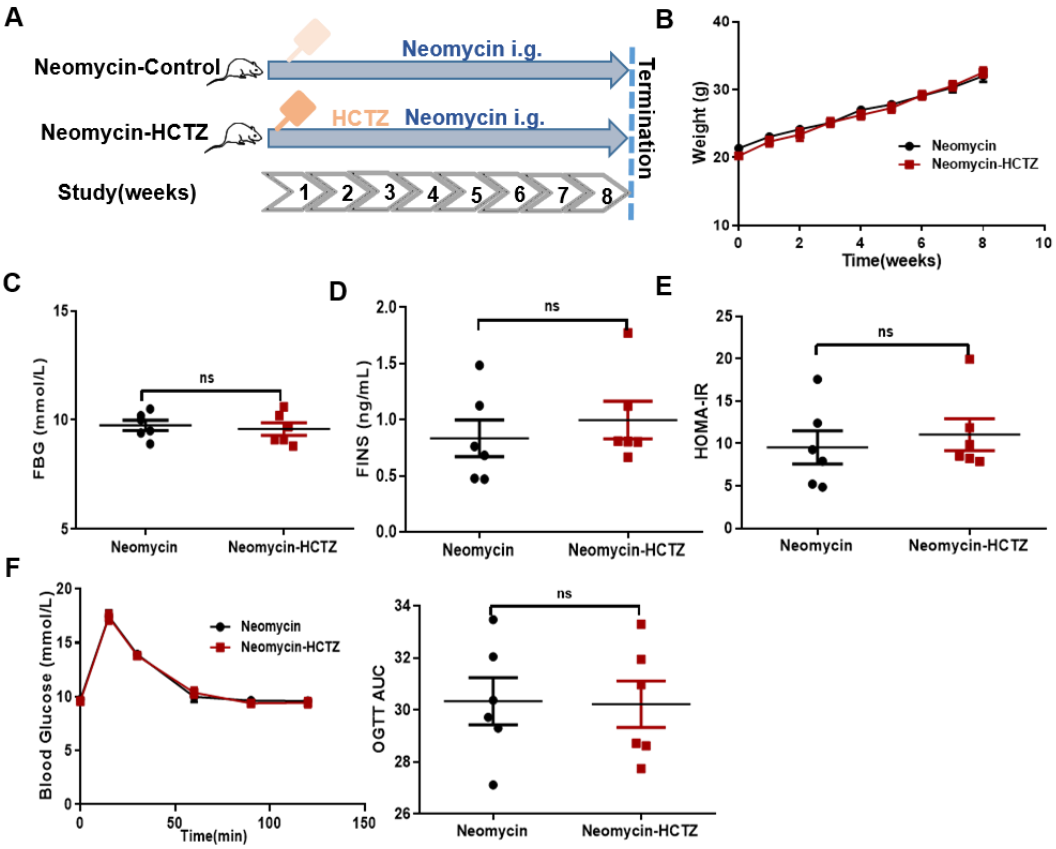

Figure S5. Neomycin treatment prevented metabolic derangements induced by HCTZ in HFD, related to Figure 4.

(A) Schematic of Neomycin-treated mice in HFD (n = 6 per group).

(B) Weight, (C) FBG, (D) FINS, (E) HOMA-IR, (F) OGTT and OGTT-AUC of Neomycin-treated mice in HFD (n = 6 per group).

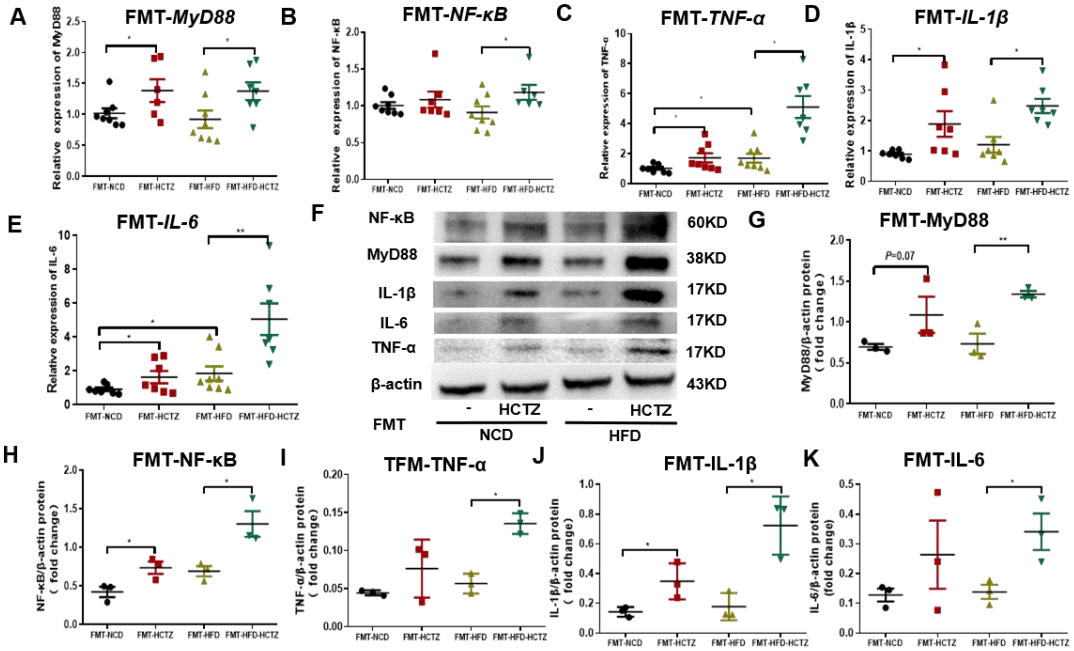

Figure S6 HCTZ causes hepatic macrophage polarization and inflammation through a TLR4-dependent mechanism, related to Figure 5.

(A)-(E) Relative *MyD88* (A), *NF-κB* (B), *TNF-α* (C), *IL-1β* (D) and *IL-6* (E) expression in liver of recipient mice in FMT (n = 6-8 per group).

(F) Representative Western blots and quantification of MyD88 (G), NF-κB (H), TNF-α (I), IL-1β (J) and IL-6 (K) levels in liver of recipient mice in FMT (n = 3-4 per group).

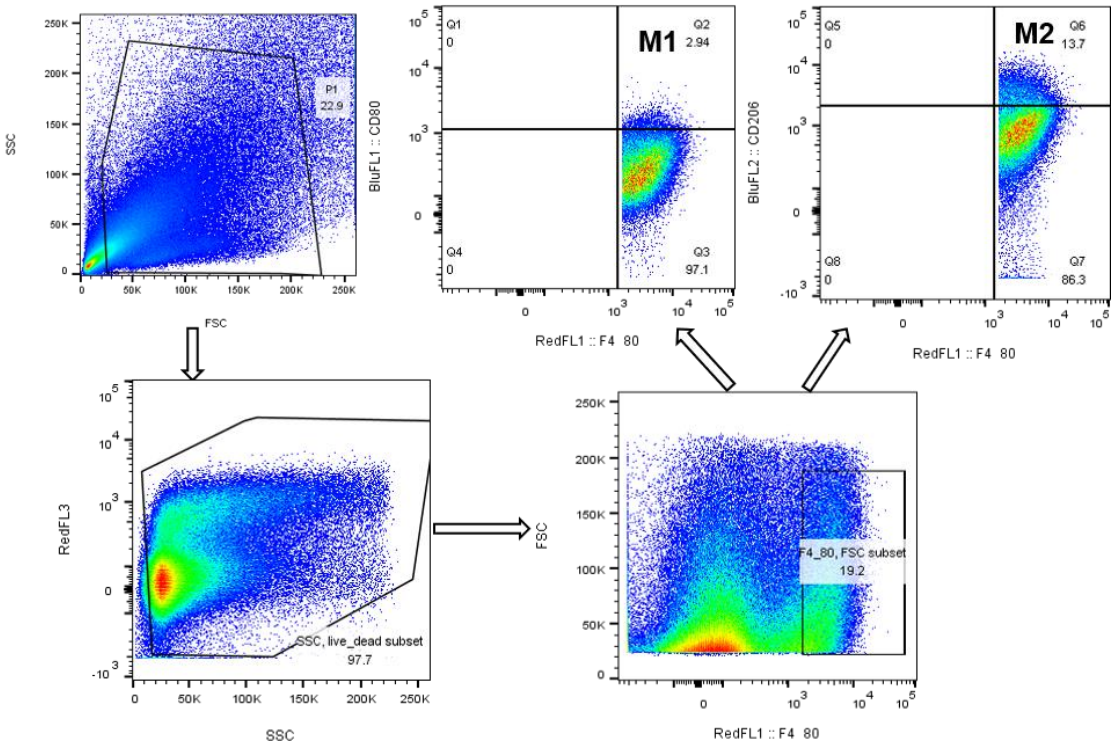

Figure S7. Gating strategy for analysis of different subpopulations of macrophages, related to Figure 5.

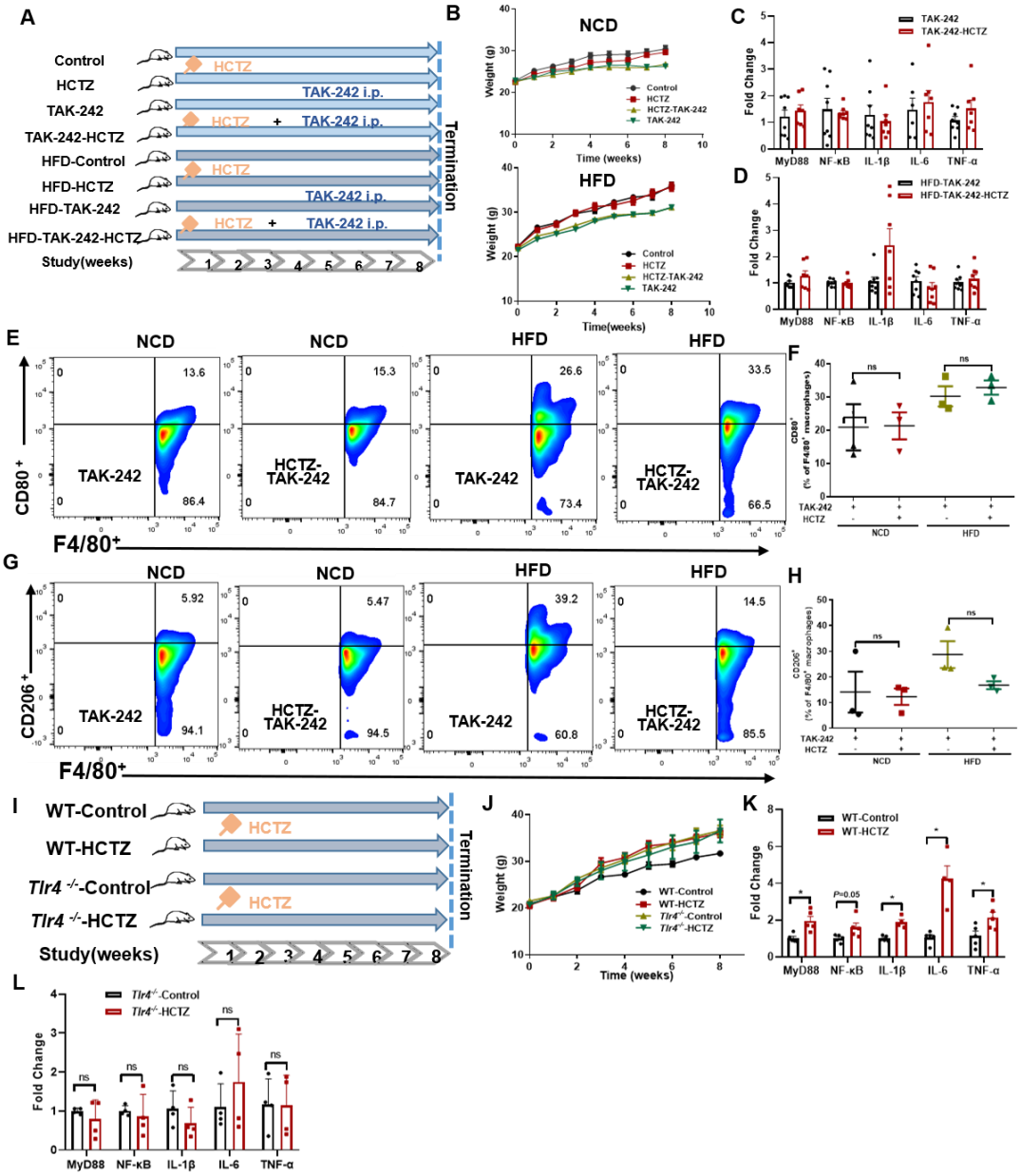

Figure S8. Pharmacologically and genetically blocking TLR4 signaling abolished HCTZ-induced macrophage polarization and inflammatory effects in liver, related to Figure 6. (A) Schematic and (B)weight of mice treated with TLR4 inhibitor TAK-242 and HCTZ (or vehicle control) (n = 6-8 per group); (C) and (D) Relative *MyD88, NF-κB, TNF-α, IL-1β* and *IL-6* expression in liver in mice treated with TLR4 inhibitor TAK-242 and HCTZ (or vehicle control) in NCD (C) and HFD (D) (n = 6-8 per group); (E) Representative CD80 staining of hepatic F4/80$^+$ macrophages in mice treated with TLR4 inhibitor TAK-242 and HCTZ (or vehicle control); (F) Flow cytometry analysis of CD80$^+$-F4/80$^+$macrophages (n = 3-4 per group); (G) Representative CD206 staining of hepatic F4/80$^+$ macrophages in mice treated with TLR4 inhibitor TAK-242 and HCTZ (or vehicle control); (H) Flow cytometry analysis of CD206$^+$-F4/80$^+$macrophages (n = 3-4 per group); (I) Schematic and (J)weight of WT or *Tlr4*$^{-/-}$ mice treated with HCTZ or vehicle control (n = 4-5 per group); (K) and (L) Relative *MyD88, NF-κB, TNF-α, IL-1β* and *IL-6* expression of WT or *Tlr4*$^{-/-}$ mice treated with HCTZ or vehicle control (n = 4-5 per group).

Supplementary Table

Table S1. Sequences of primers, related to Figures 3-6.

Gene	Sequence
GAPDH	Forward: GGTTGTCTCCTGCGACTTCA
	Reverse: TGGTCCAGGGTTTCTTACTCC
ZO-1	Forward: GCCGCTAAGAGCACAGCAA
	Reverse: GCCCTCCTTTTAACACATCAGA
Occludin	Forward: TGAAAGTCCACCTCCTTACAGA
	Reverse: CCGGATAAAAAGAGTACGCTGG
MyD88	Forward: TGCCGTCCTGTCTACATCTTTG
	Reverse: GTTGCTCAGGCCAGTCATCA
NF-κB	Forward: GCATTCTGACCTTGCCTATCT
	Reverse: CTCCAGTCTCCGAGTGAAGC
IL-1β	Forward: TCGCTCAGGGTCACAAGAAA
	Reverse: CATCAGAGGCAAGGAGGAAAAC
IL-6	Forward: TCGTGGAAATGAGAAAAGAGTTG
	Reverse: AGTGCATCATCGTTGTTCATACA
TNF-α	Forward: TCGCTCAGGGTCACAAGAAA
	Reverse: TTCGGAAAGCCCATTTGAGT